

# Determination of orotic acid in urine by capillary zone electrophoresis in tandem-coupled columns with diode array detection

Mariana Danková, Stanislav Strašík, Dušan Kaniansky\*

*Department of Analytical Chemistry, Faculty of Natural Sciences, Comenius University, Mlynská Dolina CH-2, SK-84215 Bratislava, Slovak Republic*

## Abstract

Analytical potentialities of capillary zone electrophoresis in the separation system with tandem-coupled columns to the spectral identification and determination of orotic acid (OA) in urine by diode array detection (DAD), coupled to the separation system via optical fibers, were investigated. A very significant “in-column” clean-up of OA from urine matrix was reached in the separation stage of the tandem by combining a low pH (2.8) with complexing effects of electroneutral agents [ $\alpha$ - and  $\beta$ -cyclodextrins, poly(vinylpyrrolidone) and 3-(*N,N*-dimethyldodecylammonio)propanesulfonate]. Due to this, its DAD spectral data could be acquired in the detection stage of the tandem with almost no disturbances by matrix co-migrants. The concentration limits of detection obtained under such working conditions for a 200-nl sample load of OA and 320  $\mu\text{m}$  I.D. capillary tubes were 3.5  $\mu\text{mol/l}$  (218 nm) and 0.4  $\mu\text{mol/l}$  (280 nm). Using chemometry procedures (target transformation factor analysis, fixed size moving window-evolving factor analysis, orthogonal projection approach and fixed size moving window–target transformation factor analysis) in processing of the acquired spectral data, the presence of OA in the loaded urine matrix could be confirmed with confidence when its concentration was 10  $\mu\text{mol/l}$  or slightly less.

© 2002 Elsevier Science B.V. All rights reserved.

*Keywords:* Coupled columns; Chemometrics; Orotic acid

## 1. Introduction

Orotic acid (OA), an intermediate product in pyrimidine biosynthesis, need to be determined in urine, mainly, in a context with diagnosis of inborn errors of metabolism [1–5]. The acid is present in normal human urine only at trace concentrations (e.g. recently Ševčík et al. [3] reported the value of  $0.8 \pm 0.3 \mu\text{mol/l}$  for a group of 30 healthy adults)

and it may be about  $10^3$  times higher in urine of patients having OA as a diagnostic metabolite [2–8].

Orotic acid is a relatively strong acid ( $\text{p}K_{\text{a}} \approx 1.8$  [3,9]) and, therefore, its separation and/or determination by capillary electrophoresis (CE) methods is possible within a broad pH range. The first reports dealing with the use of CE for this purpose appeared in the literature in the late 1970s. Here, capillary isotachopheresis (ITP) with photometric absorbance detection was employed in the screening for inborn errors of purine and pyrimidine metabolism [6]. ITP with conductivity detection was shown to be suitable to the determination of OA in urine and serum as well. However, it provided a low  $\mu\text{mol/l}$  detectability

\*Corresponding author. Tel.: +421-2-6029-6379; fax: +421-2-6542-5360.

E-mail address: [kaniansky@fns.uniba.sk](mailto:kaniansky@fns.uniba.sk) (D. Kaniansky).

ty for this analyte only in a combination with an ion-exchange sample clean up [4]. Capillary zone electrophoresis (CZE) with UV photometric detection [1–3,5,7,10,11] and micellar electrokinetic chromatography (MEKC) with laser-induced luminescence detection [8] offer more effective CE alternatives to a rapid determination of OA in urine than ITP. Although these techniques require no sample pretreatment at higher concentrations of OA in urine, the use of pre-column sample clean up seems essential when its determination in this matrix at a low  $\mu\text{mol/l}$  concentration level is needed [3,7]. In this context it seems appropriate to note that an effective combination of CZE with sample pretreatment as offered, for example, by the ITP–CZE combination in the column-coupling separation system, makes possible nmol/l detectabilities of OA in urine [2,12].

Wide bore (200–300  $\mu\text{m}$  I.D.) capillary tubes provide in CZE significantly lower concentration limits of detection for the analytes detectable by photometric absorbance detection [13–19] than currently preferred 50–75  $\mu\text{m}$  I.D. tubes [20]. This is apparently due to higher sample loadabilities [16] and favorable conditions in the photometric absorbance detection of the analytes in the wide bore tubes (a higher mean effective pathlength in the detection cell [20] and, at the same time, an enhanced light flux through the cell that reduces an impact of shot noise on the detection [20,21]). Therefore, it is also clear that the use of capillary tubes of larger I.D.s is advantageous in fiber optics coupled single- [22] and multi-wavelength [23] photometric absorbance detectors. For example, CZE experiments revealed [23] that a diode array detection (DAD) system coupled by optical fibers to a 320- $\mu\text{m}$  I.D. tube reached 0.2–1  $\mu\text{mol/l}$  concentration detectabilities of the CZE analytes while their identities could be confirmed with confidence when they were present in the loaded samples (200 nl) at 1–5  $\mu\text{mol/l}$  concentrations.

This work was aimed at developing a CZE procedure suitable to the spectral identification and determination of OA in urine using a DAD system connected by fiber optics to the tandem-coupled separation system [23]. Such a configuration of the separation system was favored as it allows splitting of the CZE separation into two stages in which a

sequence of favorable separation and detection conditions can be employed. For reasons mentioned above the separation system was provided with 320  $\mu\text{m}$  I.D. capillary tubes in experiments performed in this work.

## 2. Experimental

### 2.1. Instrumentation

An ITAChrom EA-101 capillary electrophoresis analyzer (J&M, Aalen, Germany) was used in this work. Its separation unit employed the tandem-coupled CZE column constructed in this laboratory [23]. The column was provided with a pair of 320  $\mu\text{m}$  I.D. (410  $\mu\text{m}$  O.D.) fused-silica capillary tubes (J&W, Folsom, CA, USA) connected in a bifurcation block [23]. The length of the first capillary of the tandem (from the injection valve to the bifurcation block) was 120 mm and the length of the second capillary (from the bifurcation block to the detector) was 70 mm. The sample was injected by a 200 nl internal sample loop of the CZE injection valve of the analyzer.

A TIDAS, multi-wavelength photometric absorbance diode array detector (J&M) was connected to the second CZE column of the tandem via optical fibers (J&M) [23]. The detector operated under the following settings: (1) scanned wavelength range: 200–350 nm; (2) integration time: 15 ms; (3) scan interval: 1.25 s; (4) number of accumulations: 80. The DAD spectral data were acquired by a Spectralys program (version 1.81, J&M). The data processing procedures used in this work included target transformation factor analysis (TTFA) [24], fixed size moving window-evolving factor analysis (FSW–EFA) [24–26], orthogonal projection approach (OPA) [24,25,27] and fixed size moving window–target transformation factor analysis (FSW–TTFA) [23]. The programs for these procedures were written in the laboratory using Mathematica for Windows (version 4.0, Wolfram, Champaign, IL, USA).

### 2.2. Electrolyte solutions and samples

Chemicals used for the preparation of the electrolyte and sample solutions were obtained from

Sigma–Aldrich (Seelze, Germany), Serva (Heidelberg, Germany), Lachema (Brno, Czech Republic) and Merck (Darmstadt, Germany).

Methylhydroxyethylcellulose 30 000 (Serva), purified on a mixed-bed ion-exchanger (Amberlite MB-3, Merck), was used as a suppressor of electroosmotic flow (EOF). It was applied in the carrier electrolyte solutions (Table 1).

Water demineralized by a Pro-PS water purification system (Labconco, Kansas City, KS, USA), and kept highly demineralized by a circulation in a Simplicity deionization unit (Millipore, Molsheim, France), was used for the preparation of the electrolyte and sample solutions. The electrolyte solutions were filtered by disposable syringe membrane filters of 0.8  $\mu\text{m}$  pore sizes (Sigma) before the use.

Urine samples, obtained from healthy adults of different diet habits and children under orotic aciduria therapy (kindly provided by J. Mannhardt, J&M) were diluted 5 times with deionized water and, at the same time, their pH values were adjusted to 2.8 by citric acid immediately after the receipt. Then they were filtered [1.2  $\mu\text{m}$  pore size filter (Millipore, Molsheim, France)] and analyzed or stored in a deep freezer at  $-15^\circ\text{C}$ . The frozen samples were melted at a room temperature and filtered before the injection into the CE equipment.

### 3. Results and discussion

#### 3.1. CZE separation in the tandem-coupled columns

As already mentioned above the CE separation system with tandem-coupled columns [23] makes possible, within certain limits, splitting of the CZE run into a sequence of the separation and detection stages. Therefore, the carrier electrolyte employed in the first (separation) stage of the run could be optimized with respect to the resolution of OA from urine matrix and requirements regarding its DAD detection could be in a certain extent ignored. On the other hand, the carrier electrolyte employed in the second (detection) stage could be chosen to reach favorable conditions in the acquisition of the spectral data while maintaining the resolution of the analyte from matrix constituents as achieved in the separation stage.

Considering acid–base properties of OA (see above) and a multicomponent and variable nature of urine matrix it is clear that the CZE separation at a low pH will be associated with minimum disturbances caused by matrix constituents. This is due to the fact that a number of matrix constituents migrating with the effective mobilities close to that of the

Table 1  
Electrolyte systems

Parameter	Electrolyte system no.			
	1	2	3	4
Solvent	Water	Water	Water	Water
Carrier anion	Phosphate	Phosphate	Phosphate	Phosphate
Concentration (mM)	10	10	10	10
Counterion	Glycine	Glycine	Glycine	Glycine
Inclusion agent 1	–	$\alpha$ -CD	$\alpha$ -CD	$\alpha$ -CD
Concentration (mM)	–	30	30	30
Inclusion agent 2	–	$\beta$ -CD	$\beta$ -CD	$\beta$ -CD
Concentration (mM)	–	10	10	10
Polymeric agent	–	–	PVP	PVP
Concentration (% w/v)	–	–	1	1
Zwitterionic agent	–	–	–	DMDAPS
Concentration (mM)	–	–	–	100
EOF suppressor	MHEC	MHEC	MHEC	MHEC
Concentration (% w/v)	0.2	0.2	0.2	0.2
pH	2.8	2.8	2.8	2.8

$\alpha$ -CD =  $\alpha$ -cyclodextrin;  $\beta$ -CD =  $\beta$ -cyclodextrin; PVP = poly(vinylpyrrolidone); DMDAPS = 3-(*N,N*-dimethyldodecylammonio)propanesulfonate; MHEC = methylhydroxyethylcellulose.

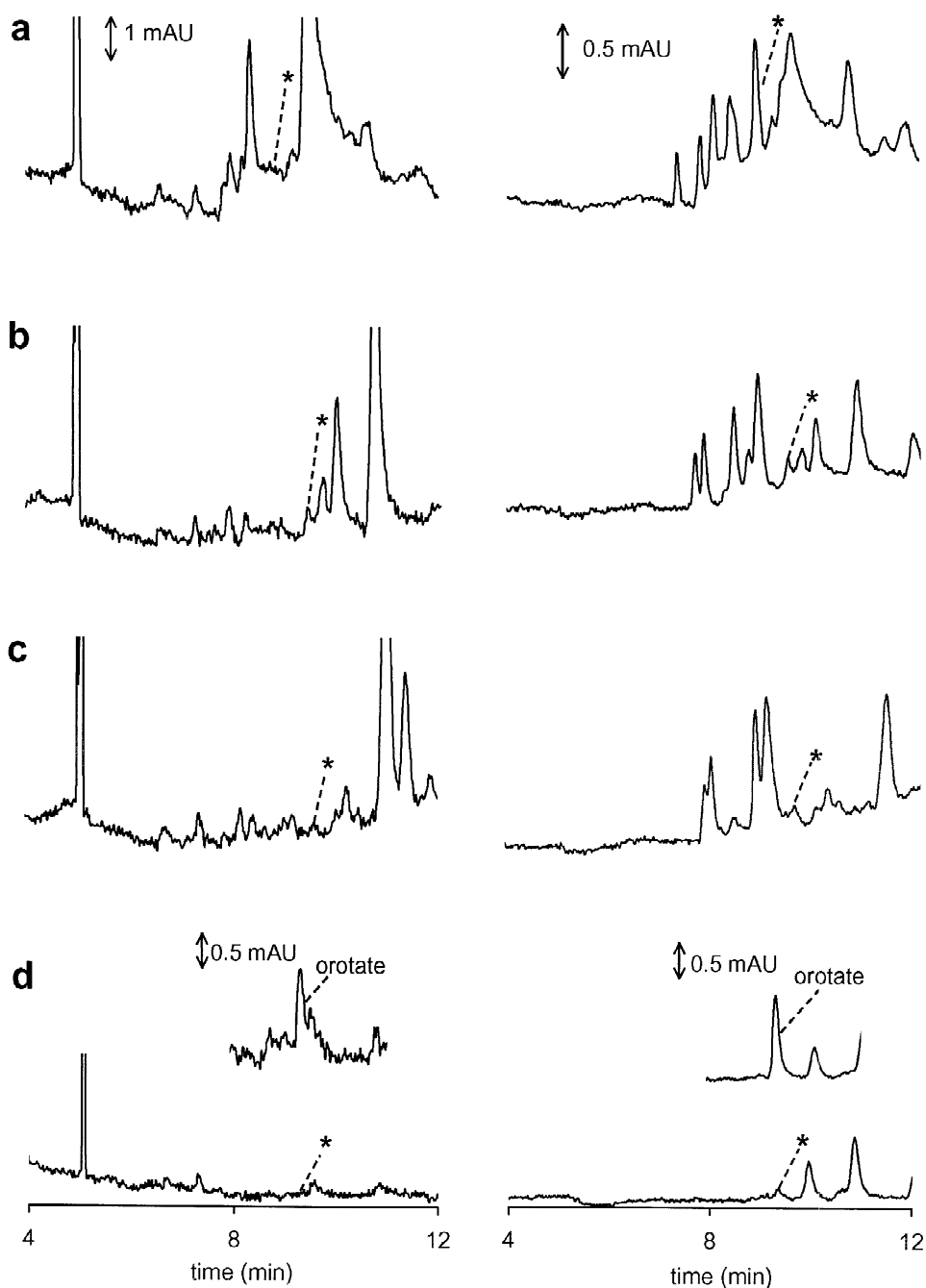


Fig. 1. Electropherograms from the CZE separations of a urine sample in the tandem-coupled columns. The electropherograms were obtained from the DAD spectral data acquired in the detection stage filled with the carrier electrolyte solution no.1 (Table 1). In the separation stage, the following combinations of the complexing additives were employed: (a) no complexing additive (system no. 1, Table 1); (b)  $\alpha$ - and  $\beta$ -CDs (system no. 2, Table 1); (c)  $\alpha$ - and  $\beta$ -CDs and PVP (system no. 3, Table 1); (d)  $\alpha$ - and  $\beta$ -CDs, PVP and DMDAPS (system no. 4, Table 1). Fragments of the electropherograms from the migration position of orotic acid (d) correspond to the run with the urine sample spiked with the acid at a  $10 \mu\text{mol/l}$  concentration. The urine sample was prepared in the way described in Section 2. The driving current was stabilized at  $120 \mu\text{A}$ .

analyte will be minimized under such acid–base conditions (a reduced risk of the overlap of the analyte peak by the matrix constituents). In fact, a majority of the works dealing with the CE determination of OA preferred such a separation mechanism [2–5,12]. We showed [12] that this separation mechanism complemented by inclusion complexations of urine matrix constituents with native cyclodextrins offers a more effective alternative in reducing matrix disturbances in the DAD detection and determination of OA. The use of these electroneutral agents is advantageous in a general sense as they do not contribute to the electric conductance of the carrier electrolyte solutions and, consequently, to thermal dispersive effects [28,29]. Therefore, our search aimed at finding separating conditions providing minimum matrix disturbances favored electroneutral agents that are known to interact with low molecular mass anionic constituents. Here, besides  $\alpha$ - and  $\beta$ -cyclodextrins we investigated separative (clean-up) effects linked with the use of poly(vinylpyrrolidone) (PVP) [17,30] and 3-(*N,N*-dimethyldodecylammonio)propanesulfonate [31–34].

Electropherograms in Fig. 1 and data in Table 2 clearly illustrate the separative (“in-column” clean-up) effects attributable to the use of the studied electroneutral agents in the carrier electrolyte solution employed in the separation stage of the tandem. They show that each of the agents contributed, although in a different extent, to the resolution of OA by reducing the effective mobilities of urine matrix constituents. It is also apparent that a maximum analytical benefit was reached when the separation was carried out in the electrolyte system

containing all these agents (Fig. 1d). Although the complexing agents could act independently, formations of multiconstituent aggregates of these agents [35] and effective interactions of the aggregates with the matrix constituents cannot be excluded. In a context of this work, however, we did not pay attention to investigations of these basic aspects of their actions. Nevertheless, electropherograms obtained from the CZE runs with urine samples of healthy adults with different diet habits (Fig. 2) and children under orotic aciduria therapy (Fig. 3) show high clean up efficiencies linked with the use of the studied agents.

### 3.2. DAD identification and quantitation of orotic acid in urine

The migration data as obtained for OA in repeated CZE runs with one of the urine samples document (Table 3) a reproducible operation of the electrolyte tandem. Analogous conclusions can be drawn from the peak height and peak area data as obtained in the same runs by DAD at preferred detection wavelengths. The recovery data (93–98% for a 10  $\mu\text{mol/l}$  concentration of the analyte) and parameters of the regression equations, describing the calibration graphs for the determination of OA at 218 and 280 nm detection wavelengths, (Table 4) complement the data relevant to its quantitation in urine.

The concentration limits of detection (cLODs) obtained for orotic acid by the present DAD, estimated from the CZE runs with a 5 times diluted urine sample (200 nl sample loads) spiked with OA at 0.2–5  $\mu\text{mol/l}$  concentrations, were 3.5  $\mu\text{mol/l}$

Table 2

Sample clean-up due to the electroneutral complexing agents present in the carrier electrolyte solutions in the separation column of the tandem

Electrolyte systems in the tandem <sup>a</sup>	Clean-up agent <sup>a</sup>	Peak area at 218 nm <sup>b</sup> (mAU s)	Peak area at 280 nm <sup>b</sup> (mAU s)
1/1	–	374	160
2/1	$\alpha$ -CD, $\beta$ -CD	310	78
3/1	$\alpha$ -CD, $\beta$ -CD, PVP	243	57
4/1	$\alpha$ -CD, $\beta$ -CD PVP, DMDAPS	69	22

<sup>a</sup> See Table 1 for the compositions of the electrolyte systems.

<sup>b</sup> A total peak area in a 7–12 min migration time interval.

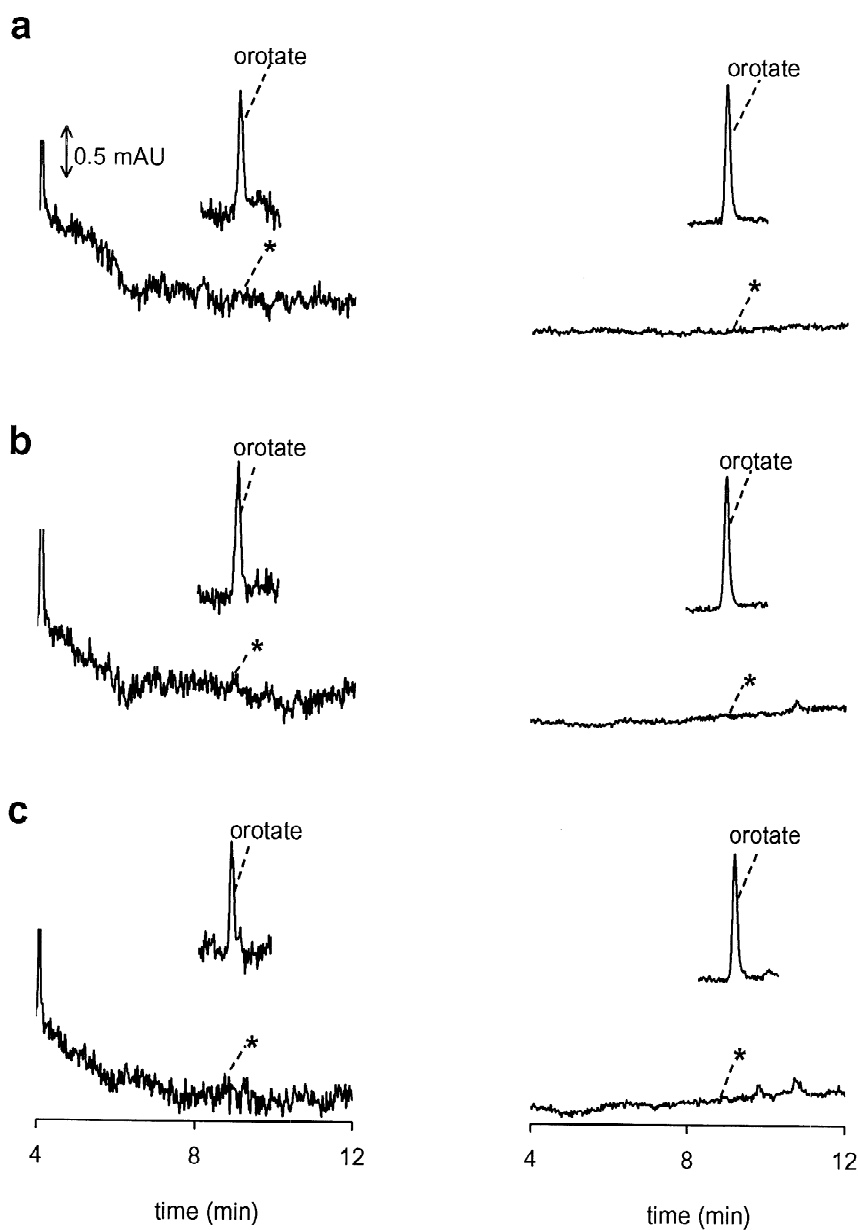


Fig. 2. Electropherograms from the CZE separations of urine samples of healthy adult volunteers with different diet habits. The electropherograms were obtained from the DAD spectral data acquired in the detection stage filled with the carrier electrolyte solution no. 1 (Table 1) while the electrolyte system no. 4 was used in the separation stage of the tandem. The migration positions of OA are marked with asterisks. Fragments of the electropherograms from its migration position correspond to the runs with the spiked samples ( $10 \mu\text{mol/l}$ ). The urine samples were prepared in the way described in Section 2. The driving current was stabilized at  $120 \mu\text{A}$ .

(218 nm) and  $0.4 \mu\text{mol/l}$  (280 nm). From the electropherograms in Figs. 2 and 3, it can be easily deduced that such differences in the detectabilities at

these wavelengths were linked, mainly, with a significantly higher noise of the present DAD detector at 218 nm. Nevertheless, these cLOD values

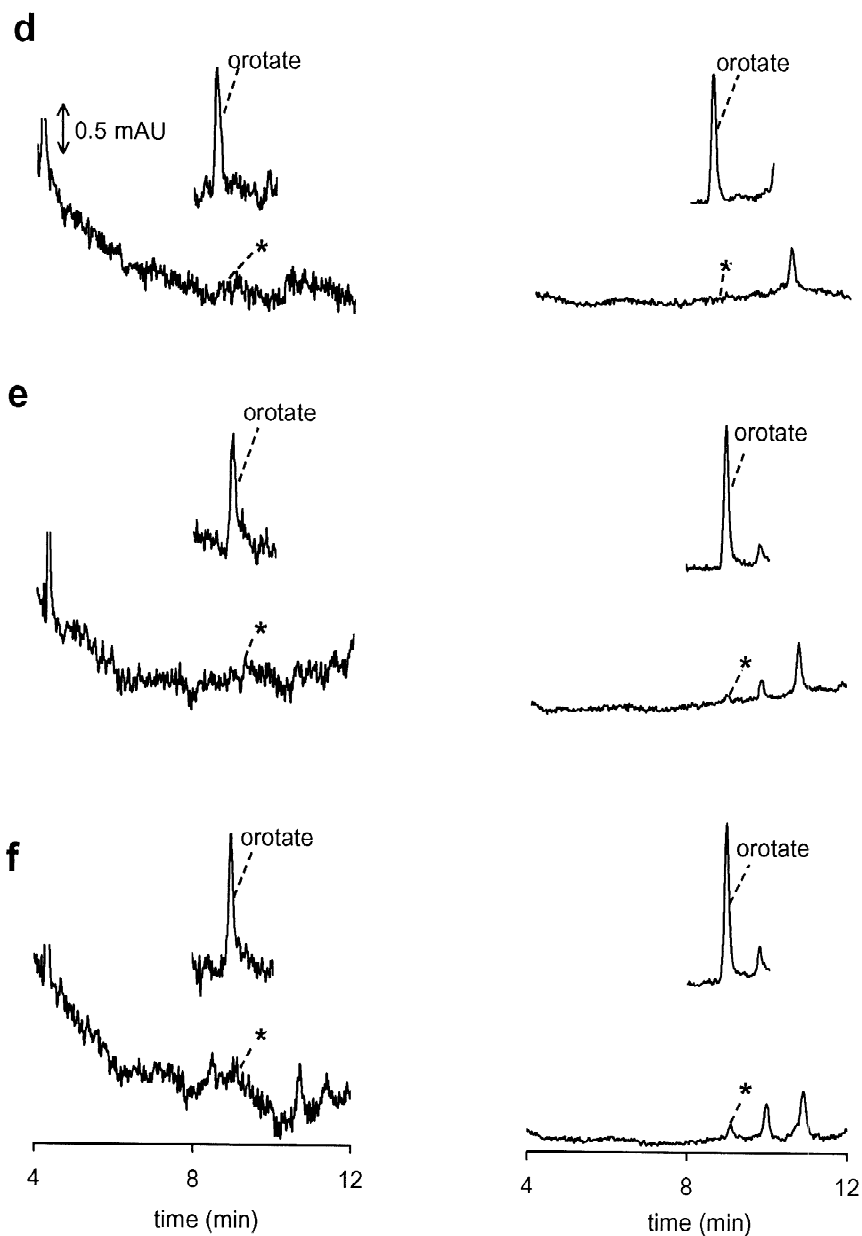


Fig. 2. (continued)

compete very well with those reported for a 75- $\mu\text{m}$  I.D. capillary tube with on-column photometric absorbance detection [3].

Electropherograms obtained from the CZE runs with one of the urine samples indicated the presence of OA at a detectable concentration (see the peaks at

218 and 280 nm marked with asterisks, in Fig. 3b). To confirm this, the spectral data from these runs were processed by chemometry procedures as employed in this work (see Section 2). The presence of orotic acid under the target peak was not confirmed by the FSW-TTFA analysis of the spectral data as

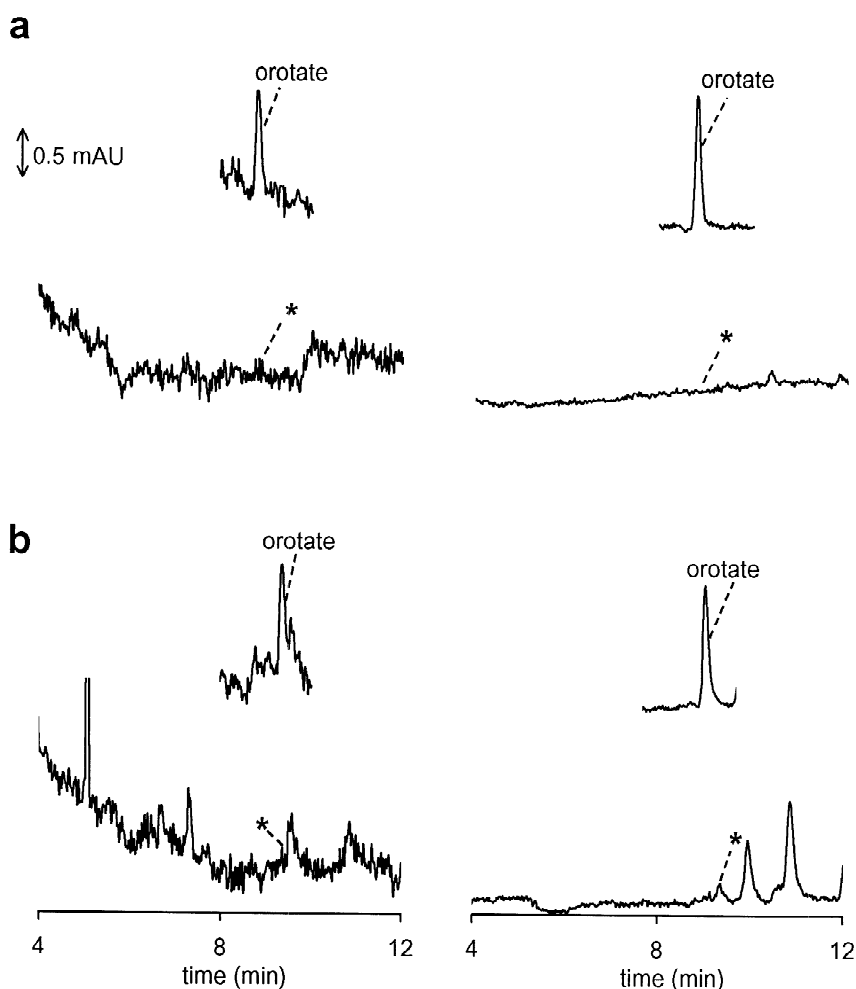


Fig. 3. Electropherograms from the CZE separations of urine samples of children under orotic aciduria therapy. The electropherograms were obtained from the DAD spectral data acquired in the detection stage filled with the carrier electrolyte solution no. 1 (Table 1) while the electrolyte system no. 4 was used in the separation stage of the tandem. The migration positions of OA are marked with asterisks. Fragments of the electropherograms from its migration position correspond to the runs with the spiked samples (10  $\mu\text{mol/l}$ ). The urine samples were prepared in the way described in Section 2. The driving current was stabilized at 120  $\mu\text{A}$ .

documented by the plot of logarithmically transformed Pearson's correlation coefficients in Fig. 4a. On the other hand, its presence was confirmed with a high certainty from the spectral data acquired from the run with the same sample spiked with OA at a 10  $\mu\text{mol/l}$  concentration (Fig. 4b). Here, a split of the OA peak on the plot can be very likely attributed to the presence of a matrix microconstituent (marked with the asterisks in Fig. 3b) in the OA peak.

A purity of the OA peak in the spiked urine was

assessed by the FSW-EFA and OPA procedures. Here, the first of the plots of the eigenvalues (E1, in Fig. 5) as obtained by FSW-EFA indicates a heterogeneity of the peak and the presence of the macroconstituent co-migrant confirms also the plot E3. Two peaks on the plot E2 can be ascribed to a spectral contribution of the carrier electrolyte and they reflect a small change in its concentration. The plot E4 and the plots of higher eigenvalues correspond to noise. The presence of the matrix microcon-



Table 3

Repeatabilities of the migration time, peak area and peak height in the CZE determination of orotic acid present at a 10  $\mu\text{mol/l}$  concentration in urine

Run no.	$t_m$ (min)	$H_{218}$ (mAU)	$A_{218}$ (mAU s)	$H_{280}$ (mAU)	$A_{280}$ (mAU s)
1	9.35	1.01	7.92	1.34	12.41
2	9.35	1.01	7.84	1.35	12.80
3	9.34	1.03	7.50	1.35	12.68
4	9.35	1.02	7.88	1.37	12.59
5	9.34	1.01	7.93	1.35	12.53
6	9.33	1.02	7.63	1.37	12.50
7	9.33	1.02	7.65	1.36	12.77
Mean	9.35	1.02	7.76	1.36	12.61
RSD (%)	0.1	0.74	2.15	0.84	1.15

$t_m$  = migration time of orotic acid;  $H_{218}$ ,  $H_{280}$  = peak height of orotic acid at 218 and 280 nm detection wavelengths, respectively;  $A_{218}$ ,  $A_{280}$  = peak area of orotic acid at 218 and 280 nm detection wavelengths, respectively.

stituent in the rear part of the analyte peak was confirmed by the OPA procedure as well (P3, in Fig. 6). The graphs P4 and P5 (Fig. 6) indicate a low concentration level of this comigrant.

#### 4. Conclusions

A sequence of the carrier electrolytes in the CZE separation system with tandem coupled columns made possible to split the analytical run into the separation of OA from urine matrix and its detection (identity confirmation) by fiber-coupled DAD. Al-

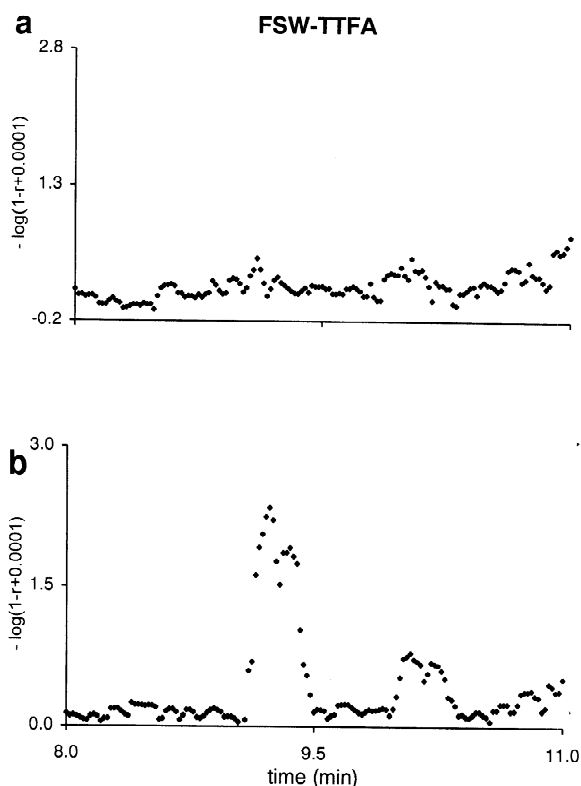


Fig. 4. Plots of logarithmically transformed Pearson's correlation coefficients from the FSW-TTFA processing of the spectral data acquired from the CZE runs with urine samples of a child under orotic aciduria therapy. The transformation used the form:  $-\log(1-r+10^{-4})$ , to prevent discontinuities in the plots for the unit values of the correlation coefficients. (a) Plot corresponding to the urine sample (the electropherogram in Fig. 3b); (b) plot for the same sample as in (a) spiked with OA at a 10  $\mu\text{mol/l}$  concentration. For further details, see the text.

Table 4

Parameters of the regression equations ( $y = a + bx$ ) for the calibration graphs of orotic acid

Detection wavelength (nm)	$a$ (mAU s)	$b$ (mAU s/ $\mu\text{mol/l}$ )	$r$	$n$
218	0.323	1.031	0.9998	21 (15)*
280	0.162	1.212	0.9996	21

The calibration data were obtained for 1–40  $\mu\text{mol/l}$  concentrations of orotic acid added to a urine sample; due to a lower detectability of OA at 218 nm only the data obtained for 7–40  $\mu\text{mol/l}$  concentrations were used (see also the text).

$y$  = peak area;  $x$  = concentration of orotic acid in the injected sample ( $\mu\text{mol/l}$ );  $a$  = intercept;  $b$  = slope;  $n$  = number of data points;  $r$  = correlation coefficient.

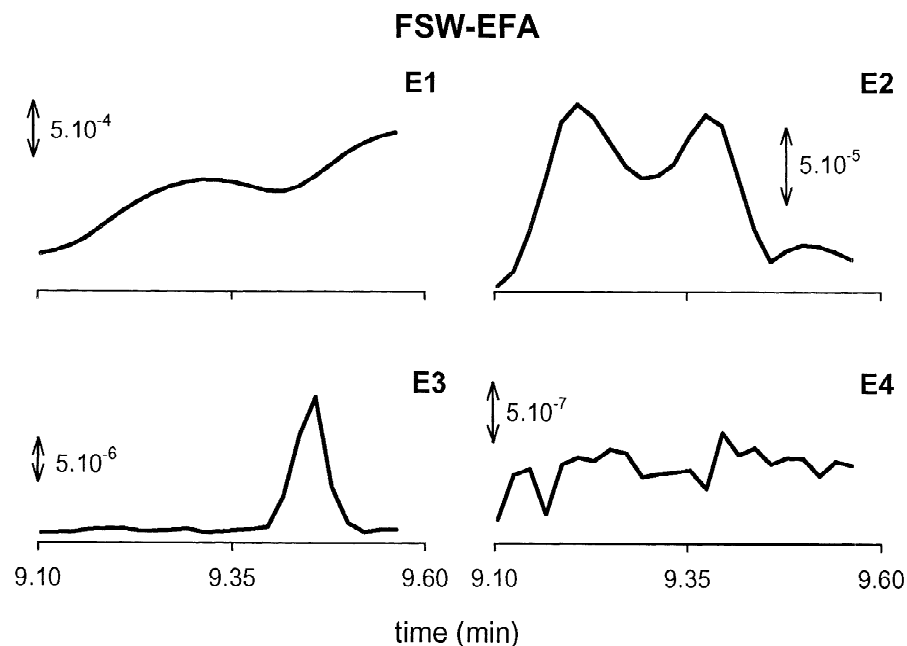


Fig. 5. Plots from FSW–EFA processing of the 3D data acquired for a urine sample of a child under orotic aciduria therapy spiked with OA at a 10  $\mu\text{mol/l}$  concentration. The sample is characterized by the electropherogram in Fig. 3b and the FSW–TTFA plot in Fig. 4b. E1–E4=time plots of the eigenvalues. For further details see the text.

though the use of wide-bore (320  $\mu\text{m}$  I.D.) tubes in the separation system did not lead to the analyte detectability as attained, under otherwise similar working conditions, by current on-column photometric absorbance detectors (see, e.g. Refs. [16–19]), an actual cLOD value reached for OA at a 280-nm detection wavelength (0.4  $\mu\text{mol/l}$ ) was still very competitive when compared to that reported for a 75- $\mu\text{m}$  I.D. tube [3].

In none of 20 urine samples taken into this study we detected the presence of OA. On the other hand, CZE experiments with these samples spiked with the analyte at a 10  $\mu\text{mol/l}$  concentration or higher (to mimic the urine samples with increased OA concentration levels) clearly revealed that using appropriate chemometry procedures to the processing of the DAD spectral data (see Section 2) we could confirm its identity with a high confidence. When a 10  $\mu\text{mol/l}$  concentration of OA is considered as a minimum at which its identity can be confirmed by the present procedure it is apparent that about 10

times higher sample load (about 500 nl of undiluted urine) is needed to make it applicable also for samples corresponding to the normal OA levels (see Section 1). Here, undoubtedly, a more practical solution is offered by the ITP–CZE combination [2,12] into which the present CZE procedure can be transferred in a straightforward way.

The use of 3-(*N,N*-dimethyldodecylammonio)propanesulfonate,  $\alpha$ - and  $\beta$ -cyclodextrins and poly(vinylpyrrolidone) in the carrier electrolyte solution employed in the separation stage of the tandem significantly contributed to the resolution of OA from urine matrix. Having no contribution to the electric conductance of the carrier electrolyte solution, these agents could be applied at high concentrations without adversely affecting the separation efficiency [28,29]. In this context, it seems logical to expect that their use as means for “in-column” sample clean-up have broader potentialities in CZE, especially, in situations when the analytes are to be determined in highly complex ionic matrices.

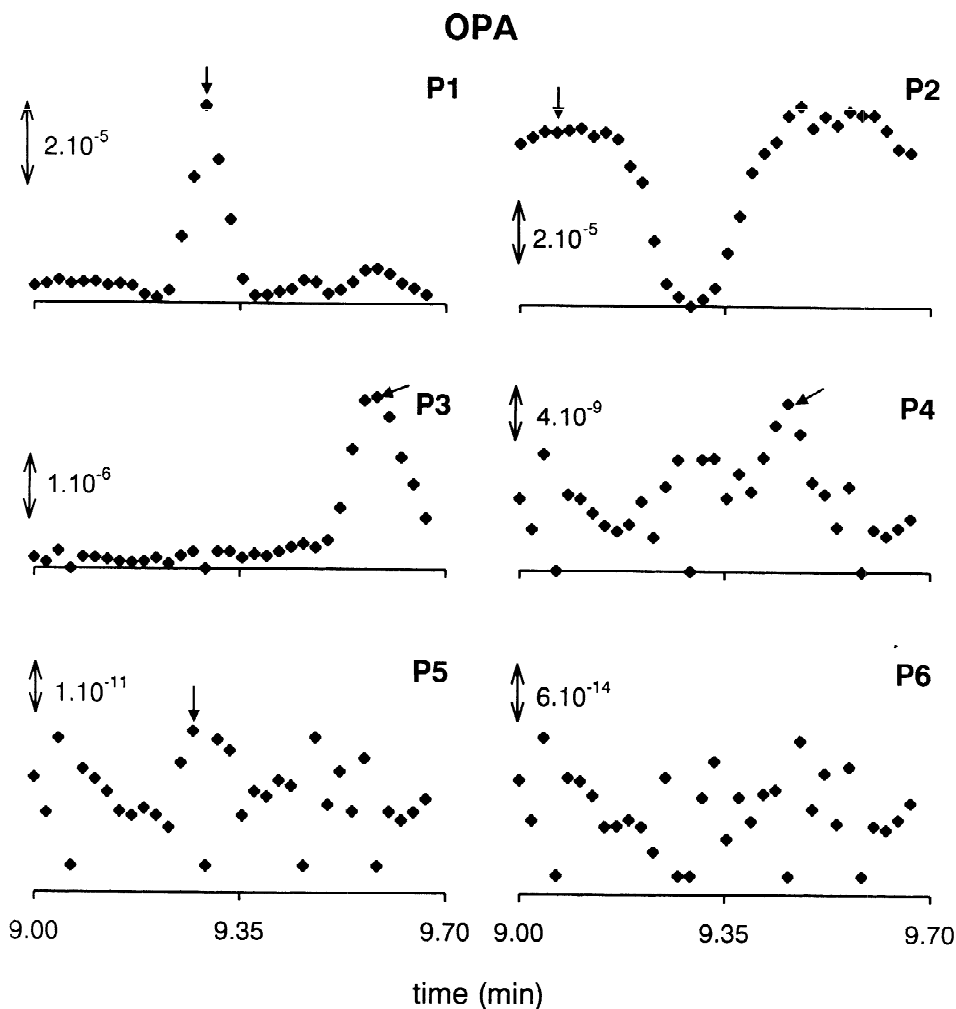


Fig. 6. Plots from OPA processing of the same 3D data as in Fig. 5. P1–P6=dissimilarity time plots. Further details are given in the text.

## Acknowledgements

This work was supported by a grant from the Slovak Grant Agency for Science under the project no. 1/7247/20. MD and SS thank for grants awarded by the Rector of Comenius University (117/2002/UK and 83/2002/UK). The authors thank to J&M (Aalen, Germany) for providing a TIDAS multi-wavelength photometric absorbance detector.

## References

- [1] E. Jellum, H. Dollekamp, A. Brunsvig, R. Gislefoss, J. Chromatogr. B 689 (1997) 155.
- [2] A. Procházková, L. Křivánková, P. Boček, J. Chromatogr. A 838 (1999) 213.
- [3] J. Ševčík, T. Adam, V. Sázel, Clin. Chim. Acta 259 (1997) 73.
- [4] T. Takechi, H. Wakiguchi, T. Kurashige, K. Kikkawa, H. Kodama, J. Chromatogr. 532 (1990) 144.

- [5] D. Friedecký, T. Adam, P. Barták, *Electrophoresis* 23 (2002) 565.
- [6] A. Sahota, H.A. Simmonds, R.H. Payne, *J. Pharmacol. Methods* 2 (1979) 263.
- [7] D.R. Franke, K.L. Nuttall, *J. Cap. Electrophoresis* 3 (1996) 309.
- [8] R. Milofsky, S. Spaeth, *Chromatographia* 42 (1996) 12.
- [9] E.M. Wooley, R.W. Wifion, L.G. Hepler, *Can. J. Chem.* 48 (1970) 3249.
- [10] E. Jellum, H. Dollekamp, C. Blessum, *J. Chromatogr. B* 683 (1996) 55.
- [11] C. Salerno, P. D'Eufemia, M. Celli, R. Finocchiaro, C. Crifo, O. Giardini, *J. Chromatogr. B* 734 (1999) 175.
- [12] M. Danková, S. Strašík, M. Molnárová, D. Kaniansky, J. Marák, *J. Chromatogr. A* 916 (2001) 143.
- [13] F.E.P. Mikkers, F.M. Everaerts, T.P.E.M. Verheggen, *J. Chromatogr.* 169 (1979) 1.
- [14] F.E.P. Mikkers, F.M. Everaerts, T.P.E.M. Verheggen, *J. Chromatogr.* 169 (1979) 11.
- [15] D. Kaniansky, M. Masár, V. Madajová, J. Marák, *J. Chromatogr. A* 677 (1994) 179.
- [16] D. Kaniansky, J. Marák, M. Masár, F. Iványi, V. Madajová, E. Šimunièová, *J. Chromatogr. A* 772 (1997) 103.
- [17] D. Kaniansky, E. Krèmová, V. Madajová, M. Masár, J. Marák, F.I. Onuska, *J. Chromatogr. A* 772 (1997) 327.
- [18] M. Masár, D. Kaniansky, *J. Cap. Electrophoresis* 3 (1996) 165.
- [19] M. Masár, D. Kaniansky, V. Madajová, *J. Chromatogr. A* 724 (1996) 327.
- [20] S.L. Pentoney, J.V. Sweedler, Optical detection techniques for capillary electrophoresis, in: J.P. Landers (Ed.), *Handbook of Capillary Electrophoresis*, CRC Press, Boca Raton, FL, 1997, p. 379, Chapter 12.
- [21] C.D. Flint, P.R. Grochowicz, C.F. Simpson, *Anal. Proc.* 31 (1994) 117.
- [22] P. Lindberg, A. Hanning, T. Lindberg, J. Roeraade, *J. Chromatogr. A* 809 (1998) 181.
- [23] S. Strašík, M. Danková, M. Molnárová, E. Ölvecká, D. Kaniansky, *J. Chromatogr. A* 987 (2003) 23.
- [24] B.G.M. Vandeginste, D.L. Massart, L.M.C. Buydens, S. De Jong, P.J. Lewi, J. Smeyers-Verbeke, *Handbook of Chemometrics and Qualimetrics. Part B*, Elsevier, Amsterdam, 1998.
- [25] K. De Braekeleer, A. de Juan, D.L. Massart, *J. Chromatogr. A* 832 (1999) 67.
- [26] J.A. Gilliard, C. Ritter, *J. Chromatogr. A* 758 (1997) 1.
- [27] A.G. Frenich, J.R. Torres-Lapasio, K. De Braekeleer, D.L. Massart, J.L.M. Vidal, M.M. Galera, *J. Chromatogr. A* 855 (1999) 487.
- [28] J.C. Reijenga, E. Kenndler, *J. Chromatogr. A* 659 (1994) 403.
- [29] F. Foret, L. Křivánková, P. Boček, *Capillary Zone Electrophoresis*, VCH, Weinheim, 1993.
- [30] D. Kaniansky, E. Krèmová, V. Madajová, M. Masár, *Electrophoresis* 18 (1997) 260.
- [31] W.Z. Hu, K. Tanaka, K. Hasebe, *Analyst* 125 (2000) 447.
- [32] M. Mori, W.Z. Hu, P.R. Haddad, J.S. Fritz, K. Tanaka, H. Tsue, S. Tanaka, *Anal. Bioanal. Chem.* 372 (2002) 181.
- [33] M.A. Woodland, C.A. Lucy, *Analyst* 126 (2001) 28.
- [34] T. Yokoyama, M. Macka, P.R. Haddad, *Anal. Chim. Acta* 442 (2001) 221.
- [35] A.M. Misselyn-Bauduin, A. Thibaut, J. Grandjean, G. Broze, R. Jerome, *J. Colloid Interface Sci.* 238 (2001) 1.